Behavior of Initiation and Growth of Creep and Creep-fatigue Small Cracks in Austenitic Stainless Steels

R. OHTANI and T. KITAMURA
Department of Engineering Science, Kyoto University, Kyoto 606, Japan

ABSTRACT

Creep tests under constant load and creep-fatigue tests under slow-fast and slow-slow strain waveforms were conducted on austenitic stainless steels. Small cracks in the fixed area of the surface of smooth specimens were observed continuously during tests or intermittently by interrupted tests. The cracks initiated successively at many grain facets being nearly perpendicular to the stress axis, and the surface length or the depth of small cracks covered a wide range from 20μm to about 1mm. The cracks were classified into two types; the propagating cracks with the coalescence and the non-propagating cracks blocked by grain boundary triple points. The propagation rates were then distributed widely for small cracks shorter than a few hundred μm. A statistical treatment showed that the mechanism of small crack growth may be the same with that of initiation and that the upper bound of the small crack propagation rate is higher than the rate predicted on the basis of the large through-crack propagation equation correlated with the creep J-integral.

KEY WORDS

Creep; creep-fatigue; small cracks; initiation and growth; austenitic stainless steels.

DISTRIBUTION OF CRACK INITIATION TIME AND CRACK LENGTH

Change in Crack Density of Creep

Figure 1 shows the change in the crack density during creep test of the coarse grained 316 stainless steel. A firstborn crack was found at the very early stage of secondary creep at the strain of less than 10%, and then the crack density increased suddenly and nearly proportionally to the time until it was saturated at the tertiary stage owing to the rapid propagation of main cracks. It was also known from other creep tests on 304 stainless steel that the increasing rate of crack density was nearly proportional to the steady state creep rate (Ohtani and Kinami, 1986).

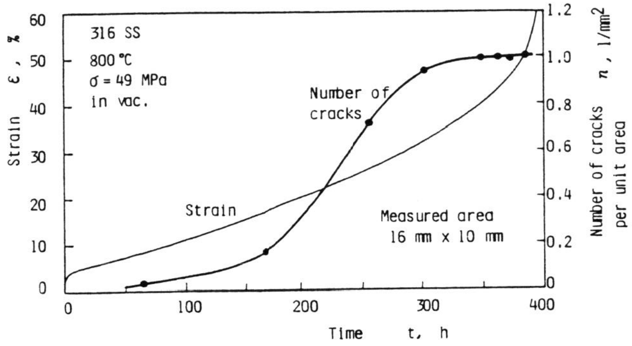

Fig.1. Change in crack density during creep in the coarse grained 316 SS.

Distribution of Crack Initiation Time in Creep-Fatigue

Histograms were obtained of the number of cracks over 20μm long or of at least one grain facet in the fixed surface area of 304 stainless steel tested under slow-fast saw-tooth strain cycle, and the results were plotted in a Weibull probability paper. They are shown in Fig.2, indicating that the initiation time can be represented by a three-parameter Weibull distribution, although the shape of distribution curve in air differs a little from that in a vacuum.

Crack-Length Distribution of Creep

The number of surface cracks was measured at the interval of surface crack length of 25μm for the fine grained 304 stainless steel. Straight lines in Fig.3 show the three-parameter Weibull distributions at the time indicated which are close to the rupture time. It is understood that the length of small cracks from the minimum 12.5μm to the maximum of about 100μm can be

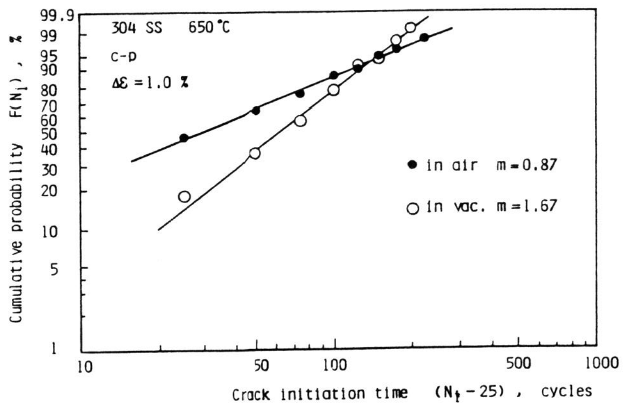

Fig.2. Weibull distribution of crack initiation time of 304 SS under slow-fast creep-fatigue, 650°C.

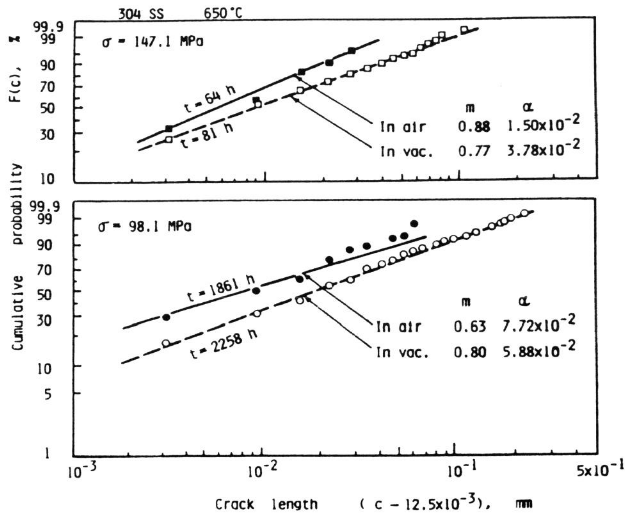

Fig.3. Weibull distributions of creep crack length.

represented by the Weibull distribution with the shape parameter of almost unity irrespective of the applied stress, loading time and test environment (Ohtani and Nakayama, 1983). This means that the small cracks do not so much act like spontaneous initiation and continuous growth but behave as continuous initiation and limited growth.

Crack-Length Distribution of Creep-Fatigue

Crack-length distributions of slow-fast creep-fatigue in the 304 stainless steel in air and in a vacuum can also be represented by a Weibull

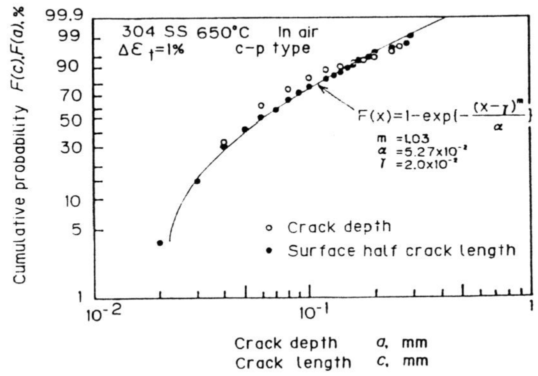

Fig.4. Weibull distributions of creep-fatigue crack length. Comparison between surface crack length and crack depth.

AFR-1—1*

distribution. Fig.4 shows the comparison between the distribution of surface crack length and that of inward crack depth. Both can be represented by the same Weibull distribution function, suggesting that the propagation rate to the inside is widely distributed in the same way as the surface propagation rate.

CRACK PROPAGATION RATE

Acceleration and Deceleration of Creep Crack Propagation

Figure 5 shows typical crack propagation curves of the coarse grained 304 stainless steel (Ohtani *et al.*, 1984). Illustrations of the propagation behavior are also shown, indicating that the wavy propagation curves are brought by the acceleration due to the coalescence to a cavity ahead of the crack or due to the lower propagation resistance after getting over a grain boundary triple point and by the deceleration usually resulting from the blockage at a triple point of grain boundaries.

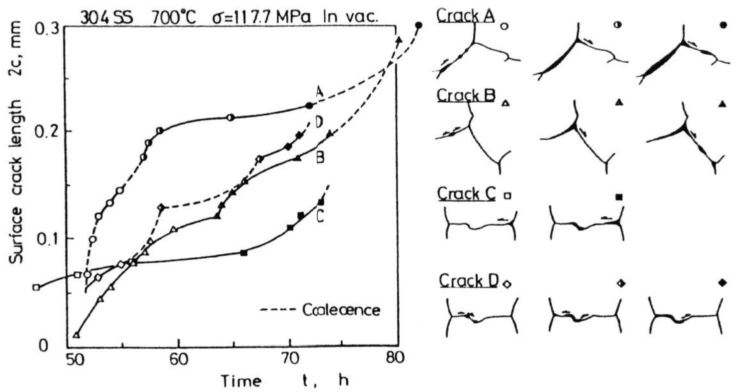

Fig.5. Typical crack propagation curves on the surface of the coarse grained 304 SS specimen in creep.

Acceleration and Deceleration of Creep-Fatigue Crack Propagation

For measuring the length of small surface cracks, the tests were interrupted at the interval of every 25 cycles and photographs were taken by an optical microscope. For the fine grained 304 stainless steel used in this test, the minimum length of the surface crack is 20μm, which corresponds to a mean length of grain-boundaries between adjacent triple points. The length of all cracks which initiated in a fixed area were measured and classified into four groups; $2c$ at N=300 (nearly the failure lifetime) is (i) more than 1mm, (ii) 0.2-1.0mm, (iii) 0.1-0.2mm and (iv) 0.02-0.1mm. Crack propagation curves of the four groups are shown in Fig.6. Cracks of the groups (i) and (ii) are propagating cracks and those of the groups (iii) and (iv) are non-propagating ones. The former is characterized by the growth being accompanied with the coalescence to the adjacent cracks. The latter is the majority of the small cracks which is blocked by grain boundaries inclined nearly perpendicularly to the crack or which is located in the shade of a longer crack.

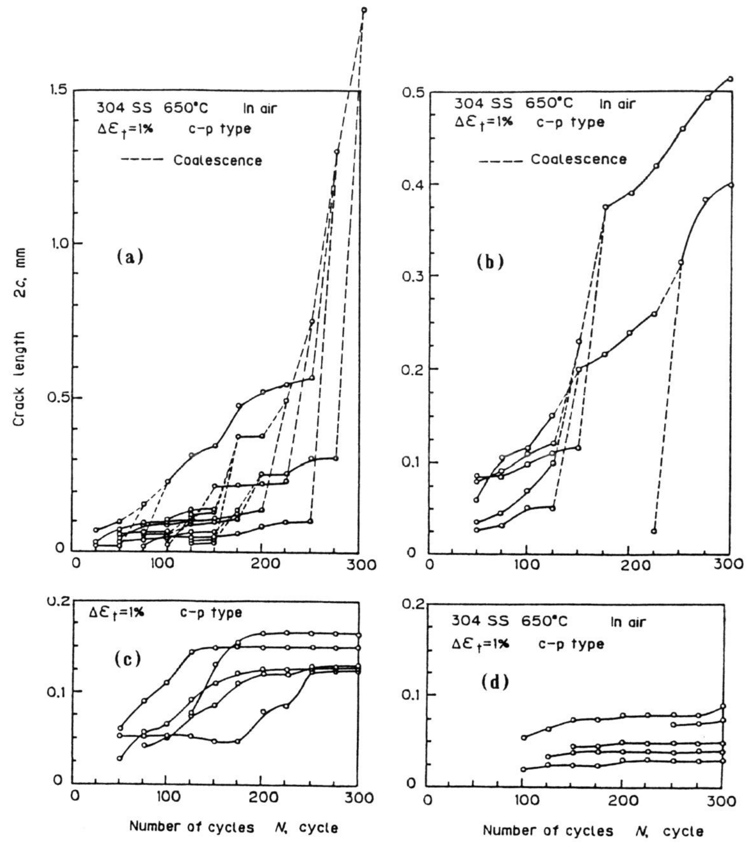

Fig.6. Crack propagation curves of 304 SS under slow-fast creep-fatigue. (a) 1mm<$2c$ (number of crack, n=1), (b) 0.2<$2c$<1mm (n=3), (c) 0.1<$2c$<0.2mm (n=8), (d) 0.02<$2c$<0.1mm (n=16).

Applicability of Creep J-integral to Creep Crack

From Fig.5 propagation rates of the four surface cracks (A-D) were estimated, and they are shown in Fig.7 as a function of crack length. Two straight lines in Fig.7 exhibit a scatter band of crack propagation rate which is predicted on the basis of the propagation law of large through-cracks of this material (Ohtani *et al.*, 1984). The propagation rate of large cracks of creep ductile materials is correlated well with the creep J-integral (Taira *et al.*, 1979, Ohtani *et al.*, 1988) and is described by the equation:

$$dl/dt\,[\text{mm/h}] = CJ^*\,[\text{kN/m h}] \qquad (1)$$

where J^* is the creep J-integral, which is given by the following equation for a small crack.

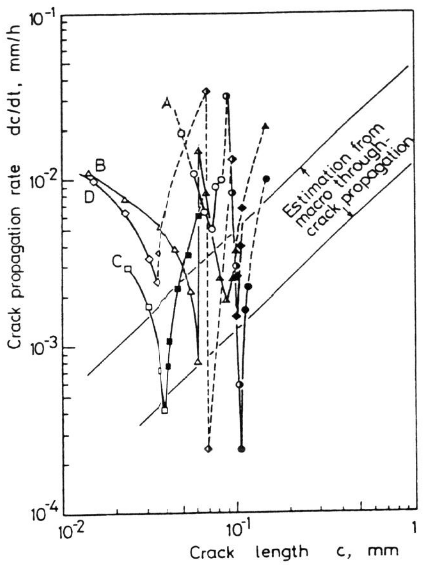

Fig.7. Propagation rates of cracks A-D of the coarse grained 304 SS in Fig.5. Two straight lines show a result predicted by the large through-crack.

$$J^* = F^2 \cdot f(n) \cdot \sigma \dot{\varepsilon}_c c \tag{2}$$

where F is the shape and boundary correction factor of the elastic stress intensity for an elliptical surface crack (ASTM STP513, 1972; STP687, 1979), and $f(n)$ is a function of creep stress exponent, n, and the following is adopted (Shih and Hutchinson, 1976).

$$f(n) = 3.85\sqrt{n}\,(1-1/n) + \pi/n \tag{3}$$

The creep deformation is expressed by a power law creep equation as

$$\dot{\varepsilon}_c\,[1/\mathrm{h}] = B\,\sigma\,[\mathrm{MPa}]^n \tag{4}$$

For the coarse grained 304 stainless steel tested at 700°C under σ=118 MPa, the material constants in Eqs.(1) to (4) are given by

$C = 1.0 \times 10^{-2}$
$F = 0.71$ for a semi-circular crack
$f(n) = 9.6$
$B = 1.3 \times 10^{-18}$, $n = 9.6$

and we can get

$$dc/dt\ [\mathrm{mm/h}] = 2.5 \times 10^{-2} c\ [\mathrm{mm}] \tag{5}$$

As can be seen in Fig.7, the propagation rate predicted by the factor of two

on dc/dt of Eq.(5) agrees roughly with or estimates slightly lower than the mean value of actual propagation rates, although the maximum and minimum values of actual propagation rates deviate beyond the bounds.

Applicability of Creep J-integral to Creep-Fatigue Crack

Large through-crack propagation of the 304 steel under slow-fast or tension stress hold cycles (so-called c-p type creep-fatigue cycle) as well as slow-slow or both tension and compression stress hold cycles (so-called c-c type creep-fatigue cycles) is time-dependent, and the propagation rates of both creep-fatigue cycles) is time-dependent, and the propagation rates of both c-p type and c-c type are described by the similar equation to the creep crack as shown by Eq.(1). Therefore, the following equation was obtained as a relation between crack propagation rate, dl/dN and creep J-integral range, ΔJ_c, where dl/dN [mm/cycle] and ΔJ_c [kN/m] are defined as time-integrals of dl/dt and J^* in one fatigue cycle (Ohtani *et al.*, 1986).

$$dl/dN = 3.0 \times 10^{-3}\,(\Delta J_c)^{1.1} \tag{6}$$

The value of ΔJ_c for a small surface crack was obtained on the basis of Eq.(2), where one-cycle time integral of the term, $\sigma\dot{\varepsilon}_c$, was estimated graphically by using a stress-strain hysteresis loop at the steady state (Ohtani *et al.*, 1981, 1986; Dowling, 1977). As the result, we got the relation between dc/dN [mm/cycle] and c [mm] for small cracks of slow-fast cycle in air

$$dc/dN = 5.9 \times 10^{-3}\,c^{1.1} \tag{7}$$

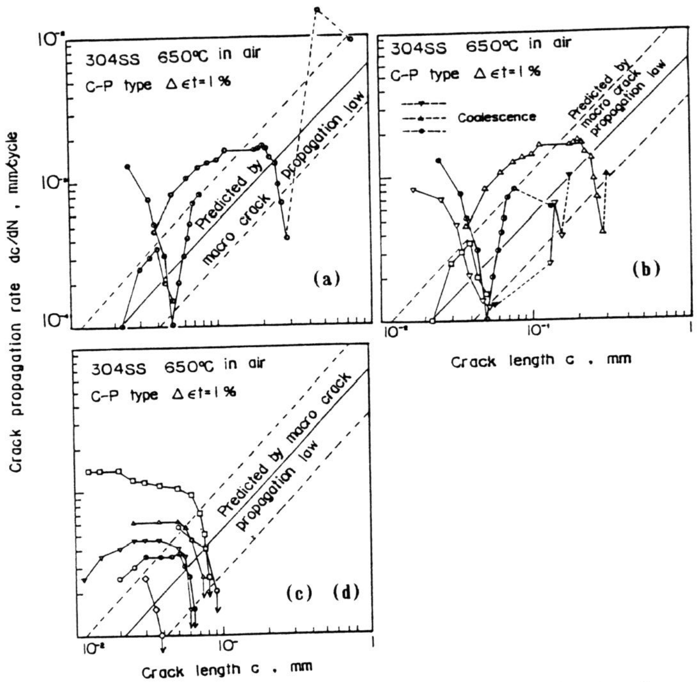

Fig.8. Creep-fatigue crack propagation rate obtained from the crack propagation curves in Fig.6.

The propagation rates of every cracks in Fig.6 were evaluated and shown as a function of crack length in the log-log diagrams of Fig.8. Solid lines in Fig.8 represent the relation of Eq.(7) and dotted lines show the bands of factor of two on crack propagation. Most of the cracks do not obey the straight line relation of Eq.(7). The length of the non-propagating cracks is less than 100μm and mostly not exceeding 50μm. The propagation rates especially for the cracks less than two or three grain boundary length are about 10 times as fast as the velocity of large cracks.

Distribution of Crack Propagation Rate

The propagation rate distributions of creep-fatigue for slow-fast (c-p type) strain waveforms in air and in a vacuum as well as for slow-slow (c-c type) in a vacuum were obtained. A result for slow-fast in a vacuum is shown in Fig.9. The value of shape parameter is about unity for each crack length except for the longest crack. Not only the length but also the initiation lifetime and the propagation rate of the distributed small cracks can be represented by Weibull probability functions of the similar form with the shape parameter of about unity. This experimental result will support the assumption that crack initiation and crack propagation are dominated by the same mechanism.

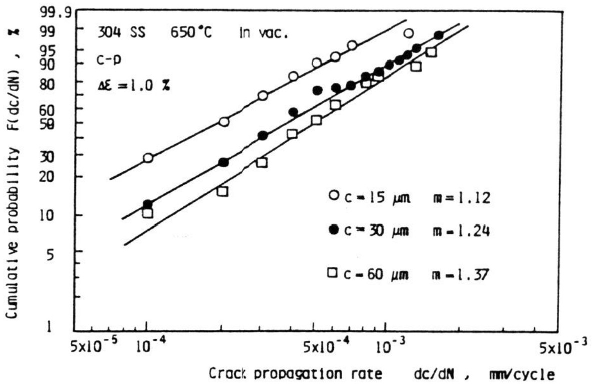

Fig.9. Weibull distribution of crack propagation rate in creep-fatigue.

ACKNOWLEDGEMENT

This work was supported by Grant in Aid for Scientific Research of the Ministry of Education, and the Funds of the Science and Technology Agency, Japan.

REFERENCES

ASTM STP 513 (1972), STP 687 (1979), American Society of Testing and Materials, Philadelphia.

Dowling, N.E. (1977). Crack growth during low-cycle fatigue of smooth axial specimens. *Cyclic Stress-Strain and Plastic Deformation Aspects of Fatigue Crack Growth, ASTM STP 637, ibid.*, 97-121.

Ohtani, R., T. Kitamura, and K. Yamada (1981). A nonlinear fracture mechanics approach to crack propagation in the creep-fatigue interaction range. *Fracture Mechanics of Ductile and Tough Materials and its Application to Energy Related Structures* (H.W. Liu, T. Kunio, V. Weiss and H. Okamura, Eds.), Martinus Nijhoff, pp.263-270.

Ohtani, R., M. Okuno, and R. Shimizu (1982). Microcrack growth in grain boundaries at the surface of smooth specimen of 316 stainless steel in high temperature creep. *J. of Society of Materials Science, Japan*, 31, 505-509.

Ohtani, R. and S. Nakayama (1983). Growth and distribution of microcracks at the surface of smooth specimen of 304 stainless steel in creep and effect of high temperature oxidation. *ibid.*, 32, 635-639.

Ohtani, R., S. Nakayama, and T. Taira (1984). Applicability of creep J-integral to microcrack propagation of creep in 304 stainless steel. *ibid.*, 33, 509-595.

Ohtani, R. and T. Kinami (1986). Nucleation, propagation and distribution of creep microcracks in 304 stainless steel. *Proc. Int. Conf. on Creep*, JSME, IMechE, ASME, ASTM, pp.167-172.

Ohtani, R., T. Kinami, and H. Sakamoto (1986). Small crack propagation in high temperature creep-fatigue of 304 stainless steel. *Trans. of JSME*, Ser.A, 52, 1825-1830.

Ohtani, R., T. Kitamura, A. Nitta, and K. Kuwabara (1988). High-temperature low cycle fatigue crack propagation and life laws of smooth specimens derived from the crack propagation laws. *Low Cycle Fatigue, ASTM STP 942*, American Society of Testing and Materials, Philadelphia, 1163-1186.

Shih, C.F. and J.W. Hutchinson (1976). Fully plastic solutions and large scale yielding estimates for plane stress crack problems. *J. of Engg. Mat. and Tech., Trans. ASME*, 98, 289-295.

Taira, S., R. Ohtani, and T. Kitamura (1973). Application of J-integral to high-temperature crack propagation, part I - creep crack propagation. *ibid.*, 101, 154-161.

Taira, S., R. Ohtani, and t. Komatsu (1979). Application of J-integral to high-temperature crack propagation, part II - fatigue crack propagation. *ibid.*, 101, 162-167.